Competition between the Stimulated Raman and Brillouin Scattering Instabilities in 0.35-μm Irradiated CH Foil Targets

H. A. Baldis
National Research Council, Ottawa, Ontario, Canada K1A0R6

P. E. Young, R. P. Drake, W. L. Kruer, Kent Estabrook, and E. A. Williams
Lawrence Livermore National Laboratory, Livermore, California 94550

T. W. Johnston
Institut National de la Recherche Scientifique–Energie, Varennes, Quebec, Canada J0L 2P0
(Received 9 August 1988)

The first experimental evidence of modification of the scattered light spectrum of stimulated Raman scattering due to the presence of significant levels of stimulated Brillouin scattering is presented. The observed spectrum, as well as the spectral *Raman gap* observed in this and other experiments, is explained in terms of the modified growth of Raman scattering in the presence of ion waves.

PACS numbers: 52.40.Nk, 52.35.Fp, 52.35.Mw

Stimulated Raman scattering (SRS) has become the most important parametric instability in laser-produced plasmas. SRS is a three-wave interaction in which the pump wave (laser light) decays into an electron plasma and a scattered light wave.[1] Apart from the intrinsic interest of SRS in laser-produced plasmas, it has important implications in inertial confinement fusion (ICF) due to the large conversion of laser energy into Raman light.[2]

An important and relatively new issue in the understanding of SRS is its growth in the presence of ion acoustic waves from stimulated Brillouin scattering (SBS). This problem has attracted considerable theoretical work[3,4] in recent years. Experiments using Thomson scattering have diagnosed the temporal evolution of electron plasma waves and ion acoustic waves associated with these instabilities, and clearly demonstrated that the growth of SRS can be modified by the presence of large levels of ion waves.[5] In those experiments, the competition between SRS and SBS was observed by directly probing the electron plasma waves and ion acoustic waves associated with the instabilities. Those experiments were performed with a much longer laser wavelength (10.6 μm) than we will be discussing here, they used preformed plasmas, and no SRS light spectrum was available.

In this paper, we present the first experimental evidence of modification of the scattered electromagnetic spectrum of SRS due to the presence of SBS, under laser-plasma conditions of interest to ICF. The time-dependent scattered spectrum shows the characteristic *Raman gap*,[6,7] with a temporal behavior that can be explained in terms of the observed SBS scattered light. The *gap* in the SRS spectrum has been seen in all published experiments; although our results do not provide a total explanation about the gap, they present an explanation consistent with the assumption of coupling or competition between the two instabilities.

The results presented in this paper were obtained during experiments using one arm of the NOVA[8] laser facility at Lawrence Livermore National Laboratory to irradiate 3-μm-thick CH foil targets with 0.35-μm light. These experiments were designed to study SRS over a large range of laser intensities (over 2 orders of magnitude), keeping the electron density gradient as constant as possible at about 1000 laser wavelengths.[9] By using constant target thickness and systematically decreasing the pulse length and spot size as the laser intensity on target increased, the changes in the electron temperature and density scale length were minimized. The laser pulse had a rise time of 100 ps and a top temporally flat to within $\pm 20\%$. As the intensity on target was increased from 10^{13} to 4×10^{15} W/cm^2, the pulse duration was decreased from 4.4 to 1 ns, the laser energy was increased from 0.6 to 2.1 kJ, and the spot size was decreased from 1100 to 250 μm. In each case the target burned through and expanded so the maximum electron density (n_e) was below 10% of the critical electron density (n_{cr}) by the end of the laser pulse.

Three diagnostics were used to obtain the data presented in this paper. The first consisted of a streak camera coupled to a spectrometer to provide time-resolved spectra of the SRS scattered light, as described previously.[9,10] The light was collected at 153° from the laser beam and 38° from the plane of polarization. A second combination of streak camera and spectrograph was used, with a special optical coupler between them. This permitted operation in six discrete channels over the spectrum with extended dynamic range, and the measurement of the scattered light within the gap region to light levels close to thermal-emission levels. A range of over 6 orders of magnitude could be recorded between the different channels. This instrument was placed at 153° from the laser beam and 71° from the plane of po-

larization. The third diagnostic measured the light backscattered into the $f/4$ focusing lens. Part of the backscattered light was sampled by a fused silica plate and relayed to a third spectrometer (0.05 nm resolution) and streak-camera combination. The spectrometer was set to look at frequencies near that of the incident laser light. Thus, simultaneous measurements of time-resolved spectra were obtained from both SRS and SBS.

Temporally and spectrally resolved SRS light is shown in Fig. 1 for laser intensities of 10^{15} and 10^{14} W/cm^2. The SBS backscattered light and the timing and duration of the laser pulse are also shown. At 10^{15} W/cm^2, the SRS spectrum ranges from approximately 480 to 650 nm, which corresponds to electron densities of $0.06n_{cr}$ and $0.20n_{cr}$, respectively. The short-wavelength boundary of the spectrum is due to Landau damping[6] corresponding to an electron temperature (T_e) of approximately 1 keV. As the maximum electron density within the laser focal spot decreases after the target burns through, the maximum wavelength of Raman light decreases as well. This shows as a diagonal cutoff in the streak records. At the long-wavelength side of the spectrum there is a maximum wavelength at which SRS is observed. The absence of SRS in the electron density range between $0.25n_{cr}$ and $\approx 0.20n_{cr}$ is the Raman gap discussed previously. This feature is observed for all CH-foil-taret shots [see Figs. 1(a) and 1(b)]. The Raman gap is wider for lower laser intensities. For $I=3\times10^{13}$ W/cm^2, the gap extends from $n_e=0.25n_{cr}$ to $n_e\simeq0.10n_{cr}$. A clear distinctive feature in our SRS data is that the gap closes shortly before the maximum wavelength of SRS begins to decreases, in all CH-foil-target shots at laser intensities above $I\simeq10^{14}$ W/cm^2. This shows as an indentation in the streak records, and is indicated by an arrow in Fig. 1(a).

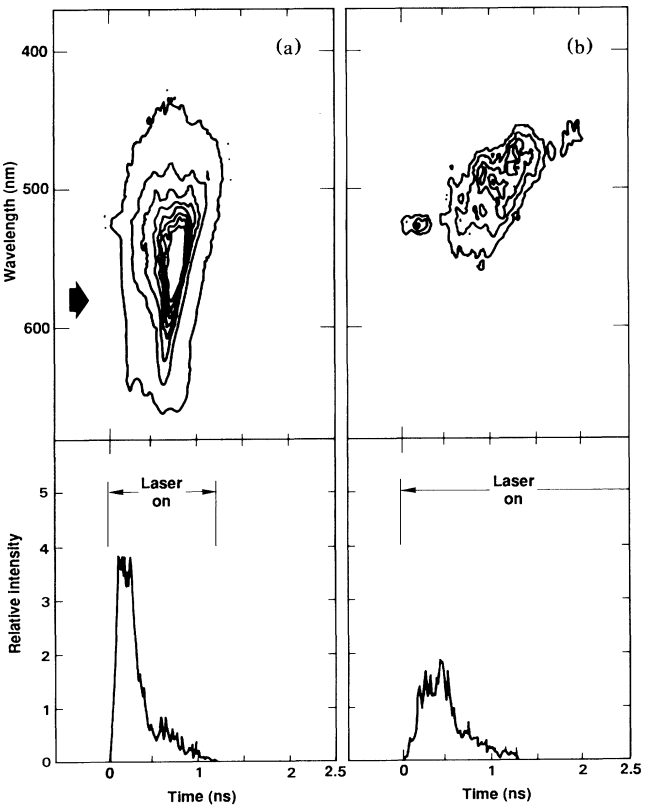

FIG. 1. Contour plots of time- and wavelength-resolved Raman intensity (top), and of time-resolved Brillouin backscattered intensity (bottom), for laser intensities of (a) 10^{15} W/cm^2 and (b) 10^{14} W/cm^2. In the Raman spectra, a timing and wavelength fiducial is seen at 530 nm. Line contours correspond to increases of approximately a factor of 3. The arrow shows the indentation in the SRS spectrum.

The wavelength-averaged time history of the SBS backscattered emission is also shown in Fig. 1. The wavelength shift is nearly constant throughout the laser pulse and is 5 Å towards the blue for $I=1\times10^{15}$ W/cm^2, and smaller for lower laser intensities.[11] It is difficult to reconcile the observed blue shift with specular reflection at n_{cr}, since simulations using the LASNEX computer code show that the n_{cr} surface is moving away from the laser at the burnthrough time. Furthermore, we have measured the backscattered wavelength shift as a function of the angle of incidence[12] and conclude, after comparison with Mach-number and density profiles generated by LASNEX, that the *peak* of the backscattered emission is produced near $n_{cr}/4$. While the location suggests that SBS is seeded by ion waves produced at $n_{cr}/4$ as a by-product of the two-plasmon decay instability,[13] we do not have enough experimental information to distinguish between this mechanism and ion turbulence. Since the backscatter emission has a broad bandwidth (≈ 10 Å FWHM), this indicates that ion fluctuations exist both above and below $n_{cr}/4$.

For the purposes of the present paper, the important feature of the backscattered emission is that the signal is brightest during the early part of the pulse, dropping to a lower level at a well-defined time. This time agrees, within 100 ps, with the burnthrough time calculated by 1D simulations using LASNEX, over a large range of laser intensities;[11] Fig. 1 shows this transition for two laser intensities. The SBS emission always shows three phases: strong SBS emission, transition time, and a lower SBS emission.

The temporal correlation between the SBS emission and the closing (or narrowing) of the gap in the spectrum of SRS for two laser intensities is shown in Fig. 1. As the level of SBS drops, SRS grows into the region of the gap, growing stronger over a large range of electron densities. For laser intensities above 10^{14} W/cm^2, this effect is observed over a large range of n_e. For lower laser intensities [Fig. 1(b)], the high level of SBS lasts longer (it takes longer for the plasma to go underdense), and the onset of SRS emission is delayed as well. For

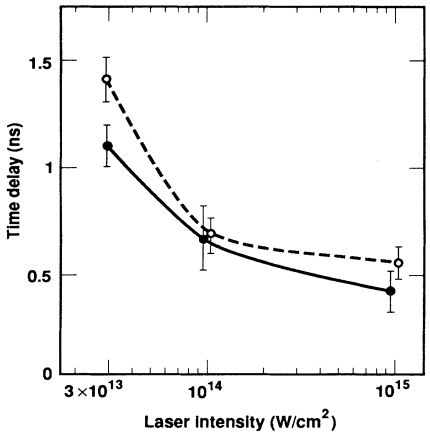

FIG. 2. Correlation between the intensity drop in the SBS backscattered light (solid line), and the beginning of the strong emission of SRS light (broken line). Time delays are measured from the beginning of the laser pulse. The vertical bars correspond to the time taken for the SBS (SRS) emission to drop (grow).

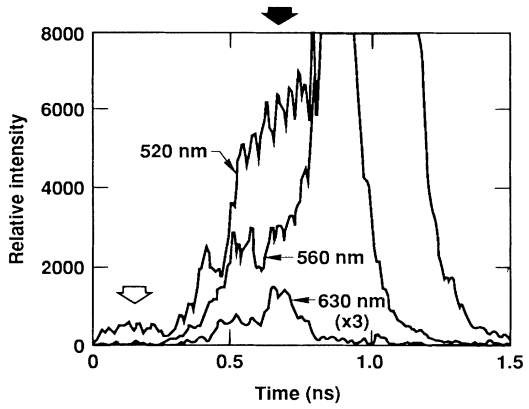

FIG. 3. Time-resolved SRS emission (in W sr^{-1} nm^{-1}) at different electron densities, for a laser intensity of 10^{14} W/cm^2: $n_e=0.09n_{cr}$ (520 nm), $n_e=0.13n_{cr}$ (560 nm), and $n_e=0.19n_{cr}$ (630 nm). Intensity of the 630-nm trace is $\times 3$. SBS emission starts at time 0. The timing of the drop in SBS emission occurs between 0.6 and 0.7 ns, and it is indicated with a black arrow. The signal before 0.3 ns for the 520-nm trace (white arrow) corresponds to a fiducial mark and is not SRS light.

$n_e < 0.10n_{cr}$, no effect of SBS on the SRS emission is observed. For $I < 10^{14}$ W/cm^2, the gap is even wider and is not seen to close, since the SRS light is observed only after the SBS light has dropped in intensity. At $I \leq 3\times10^{13}$ W/cm^2, the emission inside the gap region is thermal, which was determined by using the discrete-channel spectrometer. At this laser intensity, the emission at the maximum observed SRS (in W sr^{-1} nm^{-1}) was a factor of approximately 10^5 above the emission in the gap region. We believe the emission in the gap to be thermal subject to the uncertainties discussed in Ref. 13.

The correlation between the time delays for the transitions of SBS and SRS are shown in Fig. 2. The solid line shows the time during which the SBS light drops in intensity. The length of the vertical bars indicates the time taken for the transition. The broken line shows the time during which the SRS light intensity increases dramatically from the saturated low-level intensity (or zero intensity) observed at earlier times. There is a good correlation over 2 orders of magnitude of laser intensity.

Figure 3 shows traces of SRS intensity as a function of time for different values of n_e (SRS wavelength) at $I=10^{14}$ W/cm^2. At the highest n_e shown ($n_e=0.19n_{cr}$, $\lambda=630$ nm in Fig. 3), SRS saturates at a relatively low level (approximately 10^{-2} of the maximum observed SRS). The early saturation in the SRS light is observed over a large range of n_e (even at n_e as low as $0.13n_{cr}$, $\lambda=560$ nm in Fig. 3) while the strong SBS emission is present. At 630 nm the saturated level of SRS light corresponds to an intensity of 2×10^4 above thermal emission, or 10^{-2} of the maximum observed SRS. At higher electron densities ($\lambda=680$ nm), the SRS light saturates at an even lower level (2×10^3 above thermal emission).

Table I gives the contrast ratios I_{max}/I_{gap}, where I_{max} is the SRS emission at maximum and I_{gap} is the emission at 630 nm. At $I=10^{13}$ W/cm^2 no SRS emission is observed in the gap, and the emission is strictly thermal. At $I=10^{15}$ W/cm^2, the contrast ratio I_{max}/I_{gap} changes from 50 to 5 as the SBS emission drops in intensity. The complete absence of SRS emission near $n_{cr}/4$ at $I=10^{13}$ W/cm^2 is probably due to collisional damping. In a similar experiment using gold targets[14] instead of CH targets, complete quenching of SRS by collisional damping was observed for laser intensities up to $I=5\times10^{14}$ W/cm^2.

Once the level of ion fluctuations associated with SBS has dropped, the SRS light intensity increases over a wide range of n_e. This is particularly so in the region of higher n_e, consequently narrowing the gap. Because of the rapid evolution of n_e, the gap does not necessarily have time to fill completely. Since SRS grows strong over a large range of n_e simultaneously, we do not believe that the bright SRS emission is due to the newly created density maximum. The electron density at which SRS starts (as well as the bright Raman emission) is controlled by the level of ion fluctuations on the high-density side, and by the strong Landau damping on the low-density side.

TABLE I. Contrast ratios I_{max}/I_{gap} of the maximum SRS emission to the observed SRS in the gap (at $n_e=0.19n_{cr}$). For $I=10^{13}$ W/cm^2 the emission in the gap is thermal (see text).

	Laser intensity (W/cm^2)		
	10^{13}	10^{14}	10^{15}
Early in time (strong SBS)	10^5	125	50
Late in time (weaker SBS)	10^5	25	5

One explanation for the existence of the gap (and one that does not invoke ion waves) has been profile steepening at $n_{cr}/4$ due to the pondermotive force of plasma waves produced by the two-plasmon decay instability. As we lower the laser intensity, we would expect the profile steepening to be reduced and a narrowing of the gap to occur. In this experiment, we observed that by lowering the laser intensity by a factor of 100, the gap region, instead of narrowing, widened from less than 50 nm at $I=4\times10^{15}$ W/cm^2, to more than 200 nm at 3×10^{13} W/cm^2. This is inconsistent with the assumption of steepening at $n_{cr}/4$ being responsible for the gap.

The competition between SRS and SBS in terms of caviton formation and subsequent caviton collapse[3,15] has explained very well the National Research Council (NRC) experiments.[5] Contrary to the NRC experiment, we did not observe any short-term strong temporal modulation of SRS emission and its subsequent quenching in the presence of SBS. In the NRC experiment a preformed underdense plasma target was used, so when the laser pump was turned on both SRS and SBS had to start growing from noise level. In the experiment reported here, however, the plasma was formed by the irradiation of the laser pulse on a solid target. Consequently, the plasma conditions evolved, and by the time the threshold for SRS was reached, SBS had already grown strong. This is shown in Fig. 3, where for $n_e\approx0.20n_{cr}$, the growth of Raman scattering is observed long after SBS is fully grown.

One criterion[3,15] that can be used to identify the transition regions between SRS and SBS is the growth ratio (γ_R/γ_B). The ratio of homogeneous growth rates in the weak-coupling limit[3,16] increases as n_e decreases. This ratio of homogeneous growth rates may be also relevant to the behavior in an inhomogeneous plasma, as these growth rates enter into the threshold amplification.[1] The presence of ion fluctuations can also lead to a damping of the Raman-generated plasma wave, yielding a lower effective growth, and thus moving the transition point to even lower n_e. For example, if one assumes the wave to be coherent, a simple estimate can be given for the damping (ν_{eff}) of a plasma wave due to coupling by the Brillouin-generated ion wave into a damped plasma wave:[17]

$$\nu_{eff}\simeq\frac{\omega_{pe}}{2}\left(\frac{\delta n}{n_0}\right)^2\frac{\mathrm{Im}\epsilon}{|\epsilon(k,\omega)|^2},$$

where k is the wave number of the ion wave, $\delta n/n_0$ is the density fluctuation normalized to the background density, ϵ is the dielectric function of the plasma, and the wave number of the plasma wave has been neglected. With $\delta n/n_0\approx10\%$, this damping is sufficient to stabilize the absolute Raman instability at $0.25n_{cr}$ even for $I=3\times10^{14}$ W/cm^2. If the ion wave spectrum has a broad angular spread, the Raman-scattered light wave is also significantly damped[18] in the region near $0.25n_{cr}$ where $\omega_s\simeq\omega_{pe}$.

To summarize, we have presented clear experimental evidence for the anticorrelation of SBS and SRS in the spectral gap. We infer that the cause is the inhibition of SRS by the ion density modifications due to SBS, similar to those observed directly at longer wavelengths in preformed plasmas.

The authors acknowledge the support of E. M. Campbell and J. D. Lindl, fruitful discussions with B. F Lasinski and C. B. Darrow, and vital technical support from D. S. Montgomery and many other members of the NOVA program including those in experiments, target fabrication, and laser operations. One of the authors (H.A.B.) wants to thank D. DuBois, H. Rose, W. Rozmus, D. Villeneuve, and J. Bernard for valuable discussions. This work was performed under the auspices of the U.S. Department of Energy by Lawrence Livermore National Laboratory under Contract No. W-7405-ENG-48, with partial support (for T.W.J.) by the Ministere d'Education de Quebec and the Natural Sciences and Engineering Research Council of Canada.

[1]C. S. Liu, M. N. Rosenbluth, and R. B. White, Phys. Fluids **17**, 1211 (1974).

[2]D. W. Phillion *et al.*, Phys. Rev. Lett. **49**, 1405 (1982); R. E. Turner *et al.*, Phys. Rev. Lett. **54**, 189 (1985).

[3]C. M. Aldrich, B. Bezzerides, D. F. DuBois, and H. A. Rose, Comments Plasma Phys. Controlled Fusion **10**, 1 (1986).

[4]W. Rozmus, R. P. Sharma, J. C. Samson, and W. Tighe, Phys. Fluids **30**, 2181 (1987); H. C. Barr and F. F. Chen, Phys. Fluids **30**, 1180 (1987).

[5]C. J. Walsh, D. M. Villeneuve, and H. A. Baldis, Phys. Rev. Lett. **53**, 1445 (1984); D. M. Villeneuve, H. A. Baldis, and J. E. Bernard, Phys. Rev. Lett. **59**, 1585 (1987).

[6]W. Seka *et al.*, Phys. Fluids **27**, 2181 (1984).

[7]H. Figueroa, C. Joshi, and C. E. Clayton, Phys. Fluids **30**, 586 (1987); A. Simon, W. Seka, L. M. Goldman, and R. W. Short, Phys. Fluids **29**, 1704 (1986).

[8]E. M. Campbell *et al.*, Rev. Sci. Instrum. **57**, 2101 (1986).

[9]R. P. Drake *et al.*, Phys. Fluids **31**, 1795 (1988).

[10]R. P. Drake *et al.*, Phys. Rev. Lett. **60**, 1018 (1988).

[11]P. E. Young *et al.*, Lawrence Livermore National Laboratory, Laser Program Annual Report No. UCRL-50021-87, 1988 (unpublished).

[12]M. D. Rosen *et al.*, Phys. Fluids **22**, 2020 (1979).

[13]A. B. Langdon, B. F. Lasinski, and W. L. Kruer, Phys. Rev. Lett. **43**, 133 (1979).

[14]R. P. Drake, E. A. Williams, P. E. Young, K. Estabrook, W. L. Kruer, H. A. Baldis, and T. W. Johnston, Phys. Rev. A **39**, 3536 (1989).

[15]H. A. Rose, D. F. DuBois, and B. Bezzerides, Phys. Rev. Lett. **58**, 2547 (1987).

[16]D. W. Forslund, J. M. Kindel, and E. L. Lindman, Phys. Fluids **18**, 1002 (1975).

[17]R. J. Faehl and W. L. Kruer, Phys. Fluids **20**, 55 (1977).

[18]W. Rozmus, H. A. Baldis, and D. M. Villeneuve, Comments Plasma Phys. Controlled Fusion **12**, 1 (1988).